


Article

Study of the Mechanisms of Polymorphic Transformations in Zirconium Dioxide upon Doping with Magnesium Oxide, as Well as Establishing the Relationship between Structural Changes and Strength Properties

Alisher E. Kurakhmedov ^{1,2,*}, Aidar K. Morzabayev ², Islam Tleubay ², Askhat Berguzinov ³
and Artem L. Kozlovskiy ^{2,4} 

¹ Laboratory of Solid State Physics, The Institute of Nuclear Physics, Almaty 050032, Kazakhstan

² Engineering Profile Laboratory, L.N. Gumilyov Eurasian National University, Astana 010008, Kazakhstan; morz_a@rambler.ru (A.K.M.); itleubay@gmail.com (I.T.); kozlovskiy.a@inp.kz (A.L.K.)

³ Department of Heat Power Engineering, Toraighyrov University, Pavlodar 140000, Kazakhstan; berguzinov.a@teachers.tou.edu.kz

⁴ Department of "Chemical Processes and Industrial Ecology", Satbayev University, Almaty 050013, Kazakhstan

* Correspondence: a.kurakhmedov@inp.kz

Abstract: The aim of this work is to study the mechanisms of polymorphic transformations in ZrO₂ ceramics doped with MgO with different concentrations during thermal isochronous annealing, as well as the effect of the phase composition of ceramics on the change in strength properties and resistance to mechanical stress. Solving the problem of polymorphic transformations in zirconium dioxide by doping them with MgO will increase the resistance of ceramics to external influences, as well as increase the mechanical strength of ceramics. According to the data of X-ray phase analysis, it was found that the addition of the MgO dopant to the composition of ceramics at the chosen thermal annealing temperature leads to the initialization of polymorphic transformation processes, while changing the dopant concentration leads to significant differences in the types of polymorphic transformations. In the case of an undoped ZrO₂ ceramic sample, thermal annealing at a temperature of 1500 °C leads to structural ordering due to the partial removal of deformation distortions of the crystal lattice caused by mechanochemical grinding. During the study of the effect of MgO doping and polymorphic transformations in ZrO₂ ceramics on the strength properties, it was found that the main hardening effect is due to a change in the dislocation density during the formation of a ZrO₂/MgO type structure. At the same time, polymorphic transformations of the m—ZrO₂ → t—ZrO₂ type have a greater effect on hardening at low dopant concentrations than t—ZrO₂ → c—ZrO₂ type transformations.

Keywords: zirconium dioxide; doping; ceramics; structural materials; polymorphic transformations



Citation: Kurakhmedov, A.E.; Morzabayev, A.K.; Tleubay, I.; Berguzinov, A.; Kozlovskiy, A.L. Study of the Mechanisms of Polymorphic Transformations in Zirconium Dioxide upon Doping with Magnesium Oxide, as Well as Establishing the Relationship between Structural Changes and Strength Properties. *Ceramics* **2023**, *6*, 1164–1178. <https://doi.org/10.3390/ceramics6020070>

Academic Editor: Frank Kern

Received: 4 May 2023

Revised: 20 May 2023

Accepted: 22 May 2023

Published: 24 May 2023



Copyright: © 2023 by the authors. Licensee MDPI, Basel, Switzerland. This article is an open access article distributed under the terms and conditions of the Creative Commons Attribution (CC BY) license (<https://creativecommons.org/licenses/by/4.0/>).

1. Introduction

Interest in refractory oxide ceramics has recently been shown to be quite large due to the possibility of using them as structural materials suitable for operation under extreme conditions, such as high temperatures, radiation background, high mechanical loads, etc. [1–3]. At the same time, much attention is paid not only to the search for practical applications, as well as to the determination of the limits of applicability of refractory oxide ceramics, but also to the fundamental study of the processes of ceramic formation, as well as the relationship between methods for their preparation and modification with strength and thermophysical parameters [4,5].

In turn, among the variety of oxide ceramics, zirconium dioxide can be distinguished; the combination of thermophysical, dielectric, and insulating characteristics makes these ceramics one of the most promising in the field of reactor construction, fuel cells, and

insulators operating under extreme conditions [6–8]. However, in the case of using ceramics based on zirconium dioxide (ZrO_2) under conditions of mechanical impacts, as well as high temperatures, it is necessary to take into account the processes of polymorphic transformations that can significantly affect both the strength properties and their resistance to external influences [9–12].

As a rule, doping of ceramics based on zirconium dioxide is due to the need to increase the resistance of these ceramics to the processes of polymorphic transformations resulting from external mechanical influences, as well as thermal effects during operation [13,14]. The effect of polymorphism in these ceramics can lead to partial destruction of the strength and thermophysical parameters during long-term operation, which will adversely affect the material. The use of magnesium oxide (MgO) as a dopant, in turn, makes it possible to increase the resistance of ZrO_2 ceramics to external influences by creating additional boundary effects, as well as hardening ceramics [15–18]. At the same time, in most experiments, the concentration of the dopant varies in a fairly small range of concentrations from 0.1% to 10–15%, which is due to several factors [19,20]. Firstly, doping at low concentrations, as a rule, makes it possible to obtain ceramics of the same phase composition without the formation of new impurity inclusions in the form of dopant phases or complex oxide compounds by the type of substitution or interstitial. Secondly, low concentrations of the dopant do not give a high probability of impurity inclusions in the form of separate grains or their agglomerates, which can lead to a violation of the isotropy of the ceramic composition [21–24].

The purpose of this work is to study the effect of a magnesium oxide dopant on the processes of polymorphic transformations in ceramics based on zirconium dioxide during high-temperature annealing. The relevance of this research topic lies in the assessment of the possibility of using doping of zirconium dioxide with magnesium oxide to stabilize the phase composition and subsequent hardening of ceramics.

2. Materials and Methods

Doping of ZrO_2 ceramics with MgO oxide in order to evaluate phase polymorphic transformations in zirconium dioxide was carried out using the method of mechanochemical grinding in a planetary mill with various dopant variations from 0.01 to 0.25 molar%. ZrO_2 and MgO components of chemical purity 99.95% were used as components for the synthesis; the reagents were purchased from Sigma Aldrich (Sigma, St. Louis, MI, USA).

Ceramics were obtained using the method of mechanochemical solid-phase synthesis. A PULVERISETTE 6 classic line planetary mill (Fritsch, Berlin, Germany) was used for the synthesis. Grinding was carried out at a grinding speed of 400 rpm, and the grinding time was 60 min. For grinding, a grinding cup and balls with a diameter of 10 mm made of tungsten carbide, which has a hardness of 9 on the Mohs scale and a high level of wear resistance, were used. The ratio of grinding media and initial powders in a given molar ratio was 4:1. After grinding, the resulting powder samples were removed from the grinding jars for subsequent thermal annealing. Thermal annealing was carried out in a muffle furnace at an annealing temperature of 1500 °C for 5 h, and the heating rate was 10 °C/min. After holding the samples at a given temperature for 5 h, the samples were cooled for 24 h together with the muffle furnace. Figure 1 shows a schematic representation of the main processes for the manufacture of ceramics using the method of mechanochemical synthesis.

To compare changes in structural characteristics, and assess the possibility of initiating the processes of polymorphic transformations as a result of mechanochemical grinding and subsequent thermal annealing, a ZrO_2 powder sample with a monoclinic type of crystal structure was chosen, which is used as the main element in the preparation of doped ceramics.

Morphological features were studied using the scanning electron microscopy method performed using a Hitachi TM3030 electron microscope (Hitachi, Tokyo, Japan).

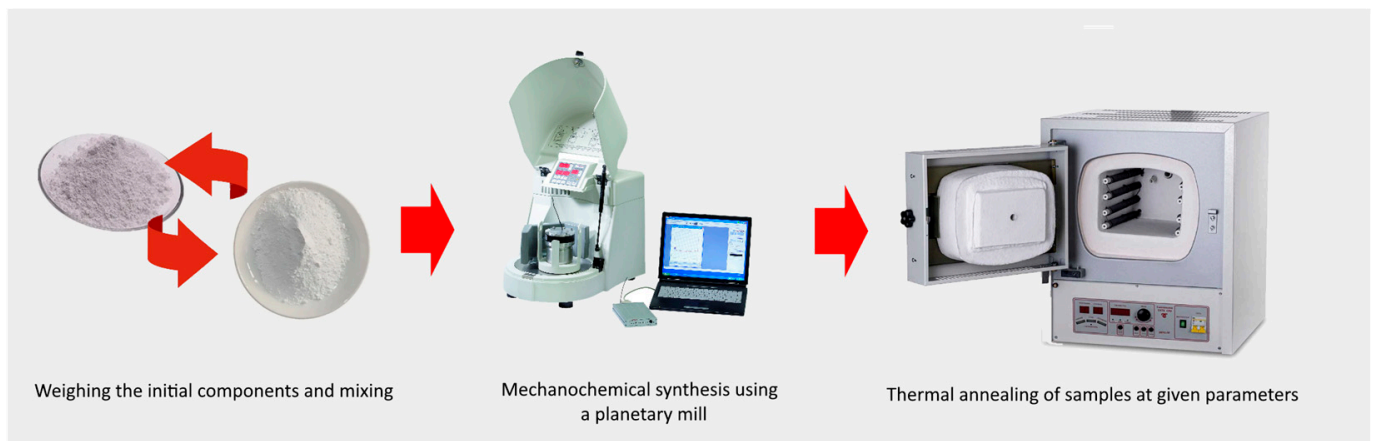


Figure 1. Scheme for obtaining ceramics.

Analysis of phase transformations associated with the processes of polymorphic transformations was carried out using the method of X-ray phase analysis. For implementation, a D8 Advanced ECO powder diffractometer (Bruker, Berlin, Germany) was used. The diffraction patterns were taken in the Bragg–Brentano geometry, in the angular range of $2\theta = 20\text{--}100^\circ$, with a step of 0.03° . The obtained diffraction patterns were analyzed in order to determine the structural parameters, as well as to establish the main phases in the composition of the ceramics. The phase composition was refined using the PDF-2(2016) database.

Determination of the strength properties was carried out by the method of intensification in order to determine the hardness values of the ceramics, as well as to establish the magnitude of the hardening of the ceramics with a change in the phase composition as a result of polymorphic transformations, as well as changes in the structural parameters. To carry out experimental work to determine the hardness values, a LECO LM700 microhardness tester (LECO, Tokyo, Japan) was used. A Vickers pyramid was used as an indenter, the load on the indenter was 100 N. The Vickers hardness value was calculated using Formula (1) [25]:

$$HV = 1.854 \frac{P}{d^2}, \quad (1)$$

where P is the applied pressure, and d is the average length of the imprint diagonal. To collect statistical data and determine the measurement error, all experiments were performed in the form of serial tests of 10–15 consecutive measurements. To measure the hardness, the samples were pressed into tablets 10 mm in diameter and 1 mm thick. Pressing was carried out at room temperature at a pressure of 300 MPa, the pressure was maintained for 30 min, after which the samples were removed for further measurements.

The hardening value was determined by assessing the change in hardness values when compared with the value characteristic of an undoped sample of ZrO_2 ceramics prepared in a similar way and annealed at a temperature of 1500°C .

3. Results and Discussion

Figure 2 shows the results of the morphological features of synthesized ZrO_2 ceramics doped with MgO with concentrations from 0.01 to 0.20 molar%. In the case of the original sample of ZrO_2 ceramics subjected to mechanochemical grinding, the morphology of the ceramics is a mixture of agglomerates of fine grains, the average size of which varies from 400 to 700 nm. At the same time, the formation of a small number of large grains of irregular rhombic shape, the average size of which exceeds $1.5\text{--}3\ \mu\text{m}$, is also observed in the grain structure. The addition of 0.01 molar% of the MgO dopant to the composition of ceramics leads to the formation of fine grains sintered into large agglomerates, which

agglomerate around large grains. Such a change may be due to effects associated with phase transformations of ceramics [26,27]. In the case of an MgO dopant concentration of 0.03 molar%, the morphology of ceramics is coarse-grained agglomerates, with a large number of boundary effects near which fine-grained inclusions are formed. At the same time, an increase in the dopant concentration to 0.05 molar% leads to grain compaction, as well as the release of a fine-grained fraction on the ceramic surface or into the interboundary space. At a dopant concentration of 0.10 molar%, inclusions with a different color gradation are observed in the interboundary space, which indicates an excellent phase and elemental composition of these inclusions. It should also be noted that the concentration of such inclusions in the interboundary space increases with increasing concentration, and the effect itself resembles the formation of structures by the type of interboundary introduction of impurity phases.

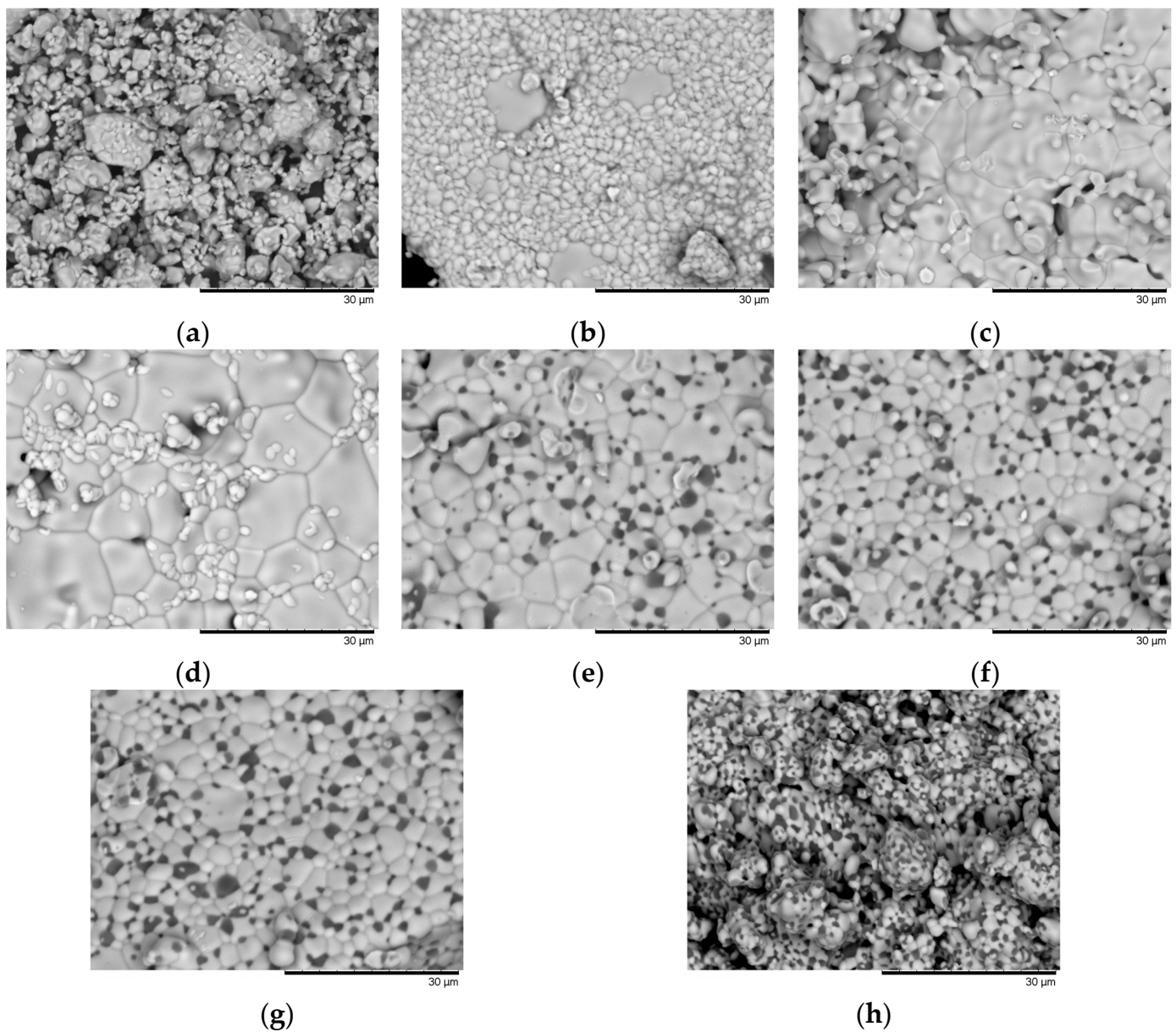


Figure 2. The results of the morphological features of the synthesized ZrO₂ ceramics depending on the concentration of the MgO dopant (a) initial; (b) 0.01 molar%; (c) 0.03 molar%; (d) 0.05 molar%; (e) 0.10 molar%; (f) 0.15 molar%; (g) 0.20 molar%; and (h) 0.25 molar%.

In a detailed analysis using the mapping method of the observed inclusions in the composition of ZrO_2 ceramics (see Figure 3), which are clearly manifested with an increase in the MgO concentration above 0.10 molar%, it was found that these inclusions are particles of magnesium oxide, the presence of which may be due to the phase transformation processes [28]. At the same time, it is clearly seen from the presented SEM image data that MgO particles are located at the grain junctions, thereby creating additional boundary effects.

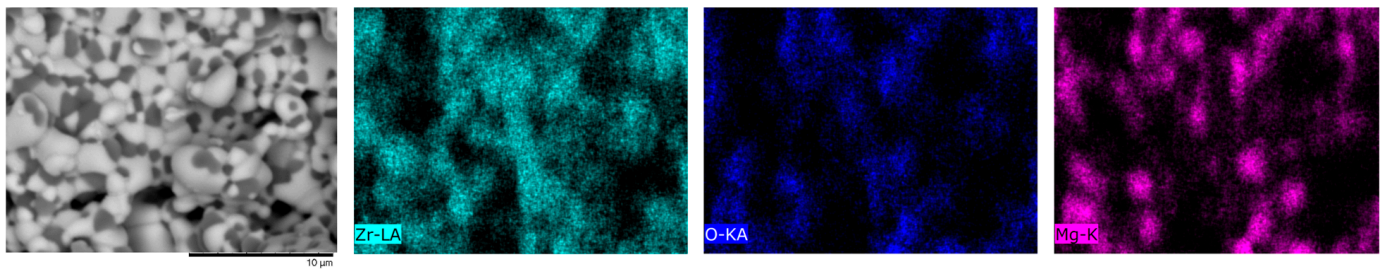


Figure 3. Mapping results reflecting the isotropy of the distribution of elements in the composition of ZrO_2 ceramics at a concentration of 0.25 molar% MgO.

Thus, analyzing the obtained data on morphological features and taking into account the mapping data, we can conclude that with an increase in the concentration of the dopant, the formation of the ceramics structure occurs according to the type of the ZrO_2 –MgO solid solution, where the main matrix is zirconium dioxide particles, with magnesium oxide particles embedded in the intergranular space, thereby forming additional boundary effects that can affect the hardening of ceramics. At the same time, an increase in the MgO dopant concentration in the composition of ceramics during thermal annealing leads to a decrease in the grain size, clearly seen in the images of Figure 2g,h, which can also affect the resistance of ceramics to mechanical and radiation damage.

Based on the obtained SEM image data, it can be concluded that an increase in the MgO dopant concentration leads to the following transformations. At low concentrations of the MgO dopant, grains recrystallize with the formation of a finely dispersed fraction, which agglomerates near the boundaries of large grains with the formation of a fairly dense packing. In the case of an increase in the dopant concentration above 0.10 molar%, a close-packed grain structure is formed, the interboundary space of which is filled with MgO grains. In the case of an increase in the MgO dopant concentration, a decrease in grain size is observed with the formation of a close-packed interstitial solid solution, which is a mixture of ZrO_2 –MgO in which the interboundary space is filled with MgO grains.

Figure 4 shows the results of X-ray phase analysis of the studied samples of ZrO_2 ceramics depending on the MgO dopant concentration. The general view of the presented X-ray diffraction patterns indicates the polycrystalline structure of the studied samples, which have a fairly high structural ordering degree, the change of which is due to the processes of polymorphic phase transformations, which are clearly manifested in the form of a change in the position of diffraction reflections with a variation in the MgO dopant concentration.

According to the presented X-ray diffraction data, thermal annealing of ZrO_2 ceramics without the addition of an MgO dopant at an annealing temperature of 1500 °C does not lead to polymorphic transformations in the form of monoclinic phase \rightarrow tetragonal phase ($m\text{-ZrO}_2 \rightarrow t\text{-ZrO}_2$) or monoclinic phase \rightarrow cubic phase ($m\text{-ZrO}_2 \rightarrow c\text{-ZrO}_2$), which consist in changing the type of crystal lattice, as well as changing the spatial synergy. Analysis of the obtained X-ray diffraction pattern for an undoped sample showed that the samples subjected to mechanochemical synthesis and subsequent thermal annealing are characterized by a monoclinic phase with a spatial synergy of $P21/a(14)$ and crystal lattice parameters of $a = 5.28894 \text{ \AA}$, $b = 5.17469 \text{ \AA}$, $c = 5.12792 \text{ \AA}$, and $\beta = 99.043^\circ$.

In this case, the difference between the obtained parameters of the crystal lattice from the reference values (PDF-00-037-1484, $a = 5.31290 \text{ \AA}$, $b = 5.21250 \text{ \AA}$, $c = 5.14710 \text{ \AA}$, and $\beta = 99.043^\circ$) is due to the deformation processes of compression (for parameters a and c) and tension (for parameter b) during mechanochemical synthesis, the presence of which is also evidenced by the distorted shape of the diffraction reflections presented in the diffraction pattern.

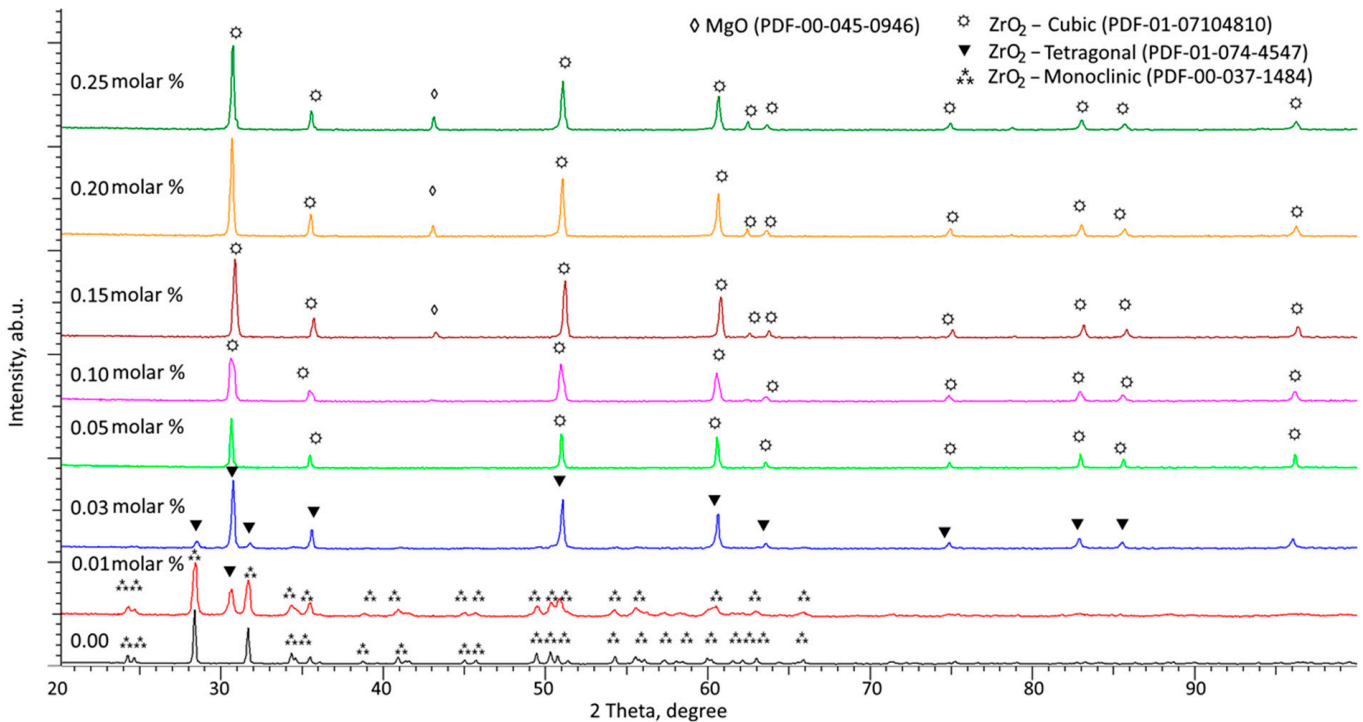


Figure 4. The results of X-ray diffraction of the synthesized ZrO_2 ceramics depending on the MgO dopant concentration.

The addition of 0.01 molar% of the MgO dopant to the composition of ceramics during mechanochemical grinding and subsequent thermal annealing leads to the formation of the tetragonal phase $t\text{-ZrO}_2$ in the composition of ceramics, the presence of which is confirmed by X-ray phase analysis data. The appearance of reflections characteristic of the tetragonal phase $t\text{-ZrO}_2$ on the diffraction pattern indicates that in the composition of ceramics during thermal annealing, the processes of polymorphic transformations of the type $m\text{-ZrO}_2 \rightarrow t\text{-ZrO}_2$ are initialized. At the same time, comparing the results of X-ray diffraction patterns of annealed ceramic samples in the initial (without the addition of MgO) state and doped ceramics, we can conclude that the presence of MgO in the powder composition leads to the initialization of polymorphic transformation processes. However, a low concentration of MgO does not allow the completion of these polymorphic transformations. According to the assessment of the weight contributions of each phase, it was found that the content of the tetragonal phase $t\text{-ZrO}_2$ is no more than 34%.

An increase in the MgO concentration to 0.03 molar% leads to the almost complete displacement of the $m\text{-ZrO}_2$ monoclinic phase, the contribution of which is estimated to be less than 10%. Such a displacement is due to the acceleration of the processes of polymorphic transformations of the $m\text{-ZrO}_2 \rightarrow t\text{-ZrO}_2$ type, which can lead to the densification of ceramics due to a decrease in the volume of the crystal lattice and rearrangement of the crystal lattice with a change in the spatial syngony from $P21/a(14)$ (monoclinic type of structure) to $P42/mmc(137)$ (tetragonal type of structure). The dominant phase in this case is the tetragonal phase $t\text{-ZrO}_2$. At the same time, the analysis of the structural parameters indicates its densification and a decrease in deformation distortions of the crystal lattice [29,30].

At an MgO dopant concentration of 0.05 molar%, according to the presented X-ray diffraction data, a second-type polymorphic transformation $t\text{-ZrO}_2 \rightarrow c\text{-ZrO}_2$ occurs during thermal annealing, with the complete displacement of the monoclinic phases and tetragonal phases. Such a structural transformation can be explained by the processes of thermal expansion with an increase in the MgO dopant concentration, which leads to an acceleration of the polymorphic transformation processes, as well as a decrease in the temperature of their initialization.

An increase in the MgO concentration to 0.10 molar% leads to a densification of the crystal lattice, which is expressed in a decrease in the volume of the crystal lattice for the $c\text{-ZrO}_2$ cubic phase, from 132.65 \AA^3 (for a concentration of 0.05 molar%) to 128.79 \AA^3 . This densification indicates the structural densification of ceramics due to the displacement of the monoclinic and tetragonal phases, as well as a decrease in the grain size. However, the distorted form of diffraction reflections due to structural compaction may be due to the effect of reducing the size of crystallites, the average value of which for a MgO concentration of 0.10 molar% is no more than 28–33 nm. Moreover, a full-profile analysis of the obtained diffraction patterns made it possible to establish the presence of low-intensity diffraction reflections at $2\theta = 43\text{--}44^\circ$, characteristic of the cubic MgO phase of the Fm-3m(225) spatial system, the content of which is no more than 3.5%.

With an increase in the MgO concentration to 0.15 molar%, the main structural changes are associated with densification of the crystal structure, as well as an increase in the impurity cubic MgO phase from 3.5% to 7%. This indicates that at high concentrations of magnesium oxide (above 0.05 molar%), not only are the processes of polymorphic transformations of the monoclinic phase into the cubic phase completed with the formation of a transitional tetragonal phase, but also structural inclusions in the form of a cubic MgO phase are formed. The formation of which, according to the data of morphological features, occurs in the intergranular space at the grain boundary.

An increase in the MgO concentration above 0.15 molar% leads to thermal expansion of the $c\text{-ZrO}_2$ cubic phase, which is due to the processes of changing the values of the coefficients of linear and volume expansion of the crystal lattice, as well as an increase in the concentration of the MgO cubic phase in the composition of ceramics. At the same time, the analysis of deformation distortions of the crystal structure indicates a decrease in the concentration of deformation stresses in the structure of ceramics [29,30].

In the case of dopant concentrations of MgO equal to 0.25 molar%, the broadening of the main reflections can be due to the formation of inclusions of the cubic substitution phase $\text{Mg}_x\text{Zr}_{1-x}\text{O}_2$, the appearance of which is due to the effects of partial replacement of zirconium ions by magnesium ions at the sites of the crystal lattice. The differences in the crystal lattice parameters can also be explained by differences in the ionic radii of zirconium (79 pm) and magnesium (66 pm).

Table 1 presents the data of structural parameters determined by the analysis of the obtained diffraction patterns. The dynamics of changes in structural parameters reflect the processes associated with structural ordering as a result of thermal annealing, polymorphic transformation processes, and thermal broadening of the crystal lattice and its volume.

Table 1. Data on the structural parameters of the studied ZrO_2 ceramics with variation in the MgO dopant concentration.

MgO Dopant Concentration, Molar%	Phase			
	m—ZrO ₂	t—ZrO ₂	c—ZrO ₂	MgO
0	a = 5.2889 Å, b = 5.1747 Å, c = 5.1279 Å, β = 99.043°, V = 138.60 Å ³	-	-	-

Table 1. Cont.

MgO Dopant Concentration, Molar%	Phase			
	m—ZrO ₂	t—ZrO ₂	c—ZrO ₂	MgO
0.01	a = 5.2618 Å, b = 5.1645 Å, c = 5.1178 Å, β = 99.159°, V = 137.30 Å ³	a = 3.5541 Å, c = 5.1205 Å, V = 64.68 Å ³	-	-
0.03	a = 5.2278 Å, b = 5.1432 Å, c = 5.0968 Å, β = 98.945°, V = 135.37 Å ³	a = 3.5594 Å, c = 5.0429 Å, V = 63.89 Å ³	-	-
0.05	-	-	a = 5.0571 Å, V = 129.32 Å ³	-
0.10	-	-	a = 5.0501 Å, V = 128.79 Å ³	a = 4.2021 Å, V = 74.20 Å ³
0.15	-	-	a = 5.0105 Å, V = 125.79 Å ³	a = 4.1782 Å, V = 72.94 Å ³
0.20	-	-	a = 5.0399 Å, V = 128.02 Å ³	a = 4.1954 Å, V = 73.85 Å ³
0.25	-	-	a = 5.0428 Å, V = 128.24 Å ³	a = 4.1913 Å, V = 73.63 Å ³

An analysis of the change in the structural parameters of the crystal lattice depending on the MgO dopant concentration showed the following. At low concentrations, the main changes in the parameters of the crystal lattice are associated with the processes of structural ordering, as well as compaction of the crystal lattice due to the reduction in deformation distortions and stresses in the structure. At the same time, polymorphic transformations of the m—ZrO₂ → t—ZrO₂ and t—ZrO₂ → c—ZrO₂ type occurring with a change in the dopant concentration are accompanied by compaction of the samples, as evidenced by a decrease in the crystal lattice parameters. However, in the case of high MgO dopant concentrations equal to 0.20–0.25 molar%, a broadening of the parameters is observed, which is due to the processes of thermal broadening of the crystal structure and its volume as a result of a change in the magnitude of thermal vibrations. Such a difference in the change in the parameters of the crystal lattice and its volume with variation in the MgO dopant concentration can be due to the fact that at high concentrations of the dopant, the processes of polymorphic transformations of the t—ZrO₂ → c—ZrO₂ type reach the limit by displacement of the tetragonal phase and its complete transformation into a cubic one. However, the processes of structural changes associated with the addition of a dopant during thermal heating at high concentrations can lead to thermal broadening processes while maintaining the structural ordering degree, as evidenced by the data presented in Figure 5a. The structural ordering degree (crystallinity degree) was calculated by comparative analysis of the weight contributions of diffraction reflections and the area of background radiation on diffraction patterns, which is characteristic of amorphous or disordered inclusions.

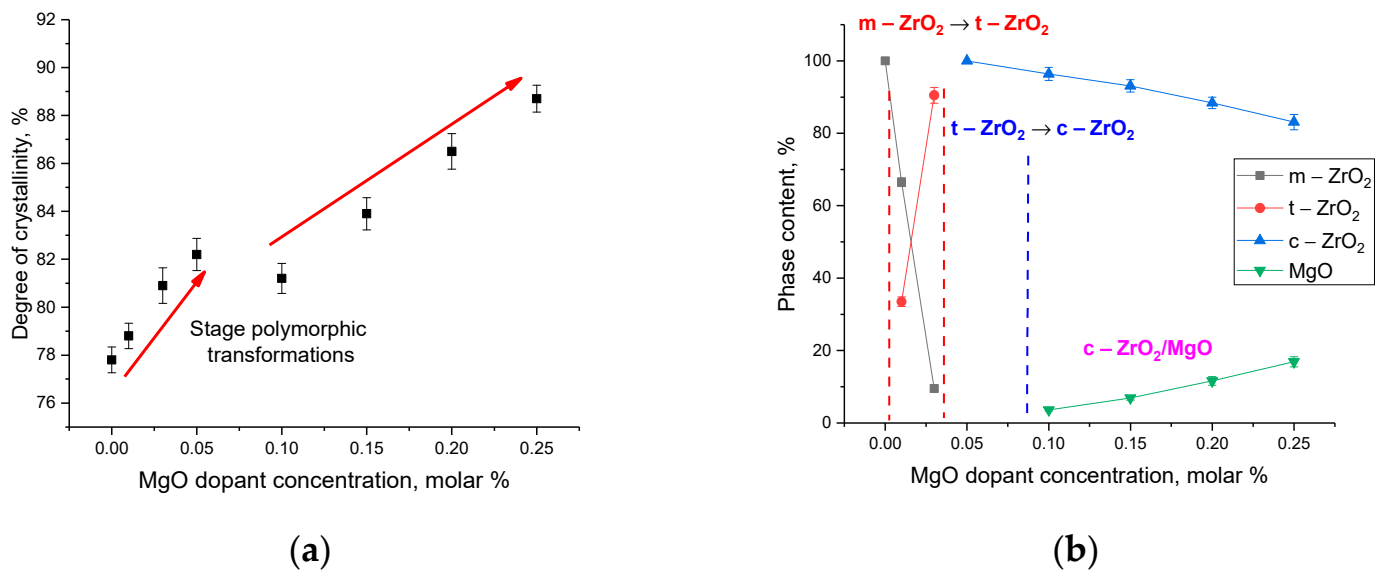


Figure 5. (a) The results of the change in the structural ordering degree (crystallinity degree) depending on the MgO dopant concentration; (b) phase diagram of polymorphic transformations in ZrO₂ ceramics with a change in the MgO dopant concentration.

The general view of the presented changes in the degree of structural ordering has a general trend towards an increase, indicating a decrease in amorphous inclusions or regions of disorder, and also confirms the above assumption about the processes of thermal broadening of the crystal lattice at MgO dopant concentrations of 0.20–0.25 molar%. The presence of a turning point at a MgO concentration of 0.10 molar% is characteristic of the formation of a cubic MgO phase in the structure of inclusions, the appearance of which at a low concentration can lead to partial disordering of the structure.

On the basis of the obtained data from the X-ray phase analysis, a phase diagram of polymorphic transformations in ZrO₂ ceramics was constructed depending on the MgO dopant concentration. The diagram is shown in Figure 5b.

The general view of the presented polymorphic transformations in ZrO₂ ceramics with a change in the concentration of the MgO dopant can be divided into three characteristic stages, accompanied by a change in the phase composition of the ceramics. The first stage is characteristic of m-ZrO₂ → t-ZrO₂ polymorphic transformations, accompanied by an increase in the concentration of the tetragonal phase with an increase in the content of the MgO dopant. The second stage is typical for polymorphic transformations of the t-ZrO₂ → c-ZrO₂ type, followed by displacement of the tetragonal and monoclinic phases, with their conversion to the cubic phase. The third stage is typical for the formation of interstitial solid solutions of the c-ZrO₂/MgO type. At the same time, the change in the dopant concentration, which leads to an increase in the contribution of the MgO phase, is in good agreement with the data of morphological studies, which reflect the filling of the interboundary space with MgO grains followed by the formation of an interstitial solid solution.

Figure 6 shows the results of changes in the density of ceramics with a variation in dopant concentration, calculated on the basis of X-ray phase analysis data, taking into account the data on changes in the parameters and volume of the crystal lattice. The density was refined taking into account the contributions of each phase, as well as changes in their structural parameters.

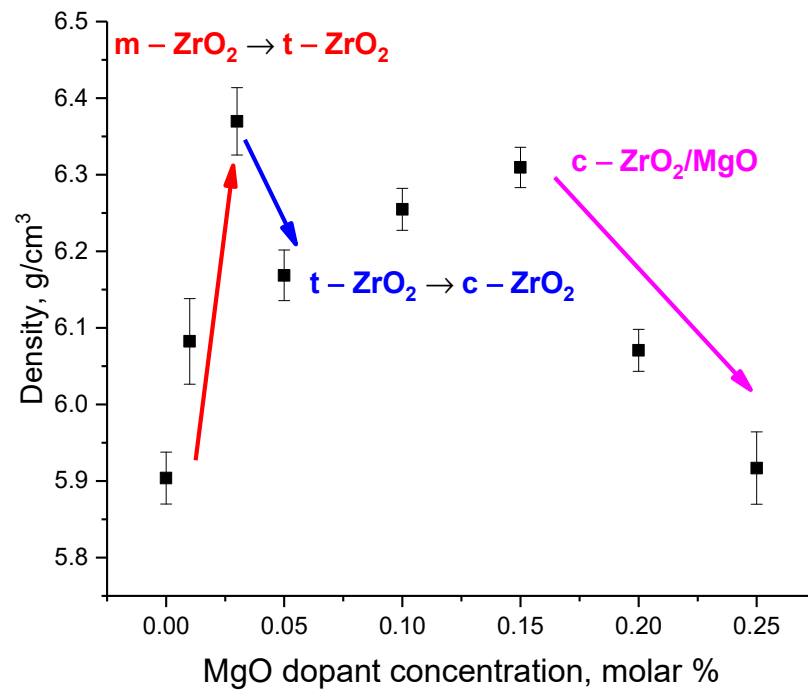


Figure 6. The results of changes in the density of ZrO₂ ceramics depending on the MgO dopant concentration.

As can be seen from the data presented, the general form of changes in density indicates a strong influence of the processes of polymorphic transformations and densification of ceramics with variation in MgO dopant concentrations. In the case of polymorphic transformations of the $m\text{-ZrO}_2 \rightarrow t\text{-ZrO}_2$ type, the displacement of the $m\text{-ZrO}_2$ monoclinic phase leads to an increase in the density of ceramics, as well as a decrease in porosity. At the same time, the dominance of the tetragonal phase in the composition leads to an increase in density to 6.36 g/cm^3 . The second type of polymorphic transformations of the type $t\text{-ZrO}_2 \rightarrow c\text{-ZrO}_2$ leads to a slight decrease in density, which is associated with the presence of impurity inclusions, as well as deformation distortions caused by phase transformations. An increase in the dopant concentration from 0.05 to 0.15 molar% leads to densification of ceramics with the dominant cubic phase in the structure, which indicates the densification and structural ordering of the crystal lattice, as well as a decrease in its volume. At the same time, the formation of inclusions in the ceramic structure in the form of a cubic MgO phase, which has a rather low density (3.56 g/cm^3), leads to a decrease in density values from 6.3 to 5.9 g/cm^3 .

An important factor in the change in polymorphic transformations in ceramics is the change in their strength and thermophysical characteristics, the change in which regulates the area of applicability of ceramics, as well as the range of possibilities for their application. Moreover, in most cases, the addition of dopants in the form of magnesium oxide or yttrium oxide is used not only to stabilize phase polymorphic transformations in ceramics, but also to increase resistance to external influences [31–33].

Figure 7a shows the results of estimating the change in the hardness of ZrO₂ ceramics depending on the concentration of the MgO dopant. The hardness was determined using the indentation method using a microhardness tester, and the measurement error was determined by collecting statistical data during serial tests.

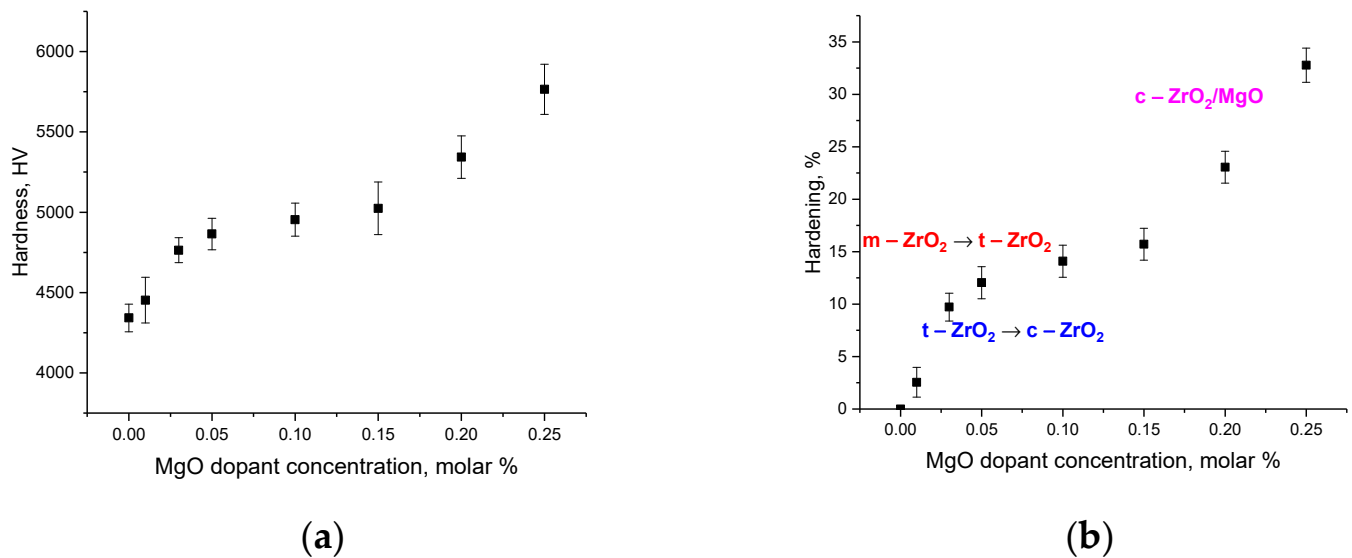


Figure 7. (a) The results of the change in the hardness value depending on the MgO dopant concentration in the composition of ceramics; (b) the results of the evaluation of the effect of hardening of ZrO_2 ceramics depending on the concentration of MgO dopant.

As can be seen from the presented data, the most pronounced changes in hardness are observed for samples that are interstitial solid solution $c\text{-ZrO}_2/\text{MgO}$, for which the hardness value is more than 5300 HV. At the same time, phase transformations of the $m\text{-ZrO}_2 \rightarrow t\text{-ZrO}_2$ type lead to greater changes in hardness, and as a result, greater hardening than subsequent phase polymorphic transformations $t\text{-ZrO}_2 \rightarrow c\text{-ZrO}_2$, for which the change in hardness is minimal (no more than 1–2%). Figure 7b shows the results of the change in hardening value calculated from these changes in hardness values compared with an undoped ZrO_2 ceramic sample obtained under the same conditions.

As can be seen from the presented data, polymorphic transformations of the $m\text{-ZrO}_2 \rightarrow t\text{-ZrO}_2$ type lead to hardening with ceramics by 3–10% with the displacement of the monoclinic phase from the composition of ceramics and the dominance of the tetragonal phase. In this case, polymorphic transformations of the $t\text{-ZrO}_2 \rightarrow c\text{-ZrO}_2$ type lead to an increase in the hardening value from 9.7% to 12%, and further structural ordering of the cubic phase leads to an insignificant change in the hardening value (no more than 1.5–3%). At the same time, the maximum increase in strength above 15% is observed for samples in which the formation of intergranular inclusions occurs in the form of a cubic MgO phase, as well as a decrease in grain size (see Figure 2). Such a difference in the effects of hardening may be due to differences in the effects caused by a change in the concentration of the dopant in the composition of ceramics, as well as the processes associated with them. The reduction in grain sizes during recrystallization leads to an increase in the number of boundary effects, as well as dislocation density, which has a direct relationship with the change in grain sizes. As is known, the value of the dislocation density is inversely proportional to the square of the average value of the grain sizes, from which it follows that a decrease in the grain size leads to an increase in the dislocation density. At the same time, variation in dislocation density at its increase can lead to the occurrence of hardening effects due to the creation of additional obstacles to the propagation of microcracks and cleavages under external actions, including indentation, which is an effect of the indenter on the sample surface at constant pressure during certain time intervals [32,33].

Figure 8a shows the results of estimating the change in the dislocation density depending on the MgO dopant concentration. The dislocation density was estimated using the grain size estimate presented in the SEM images of Figure 2.

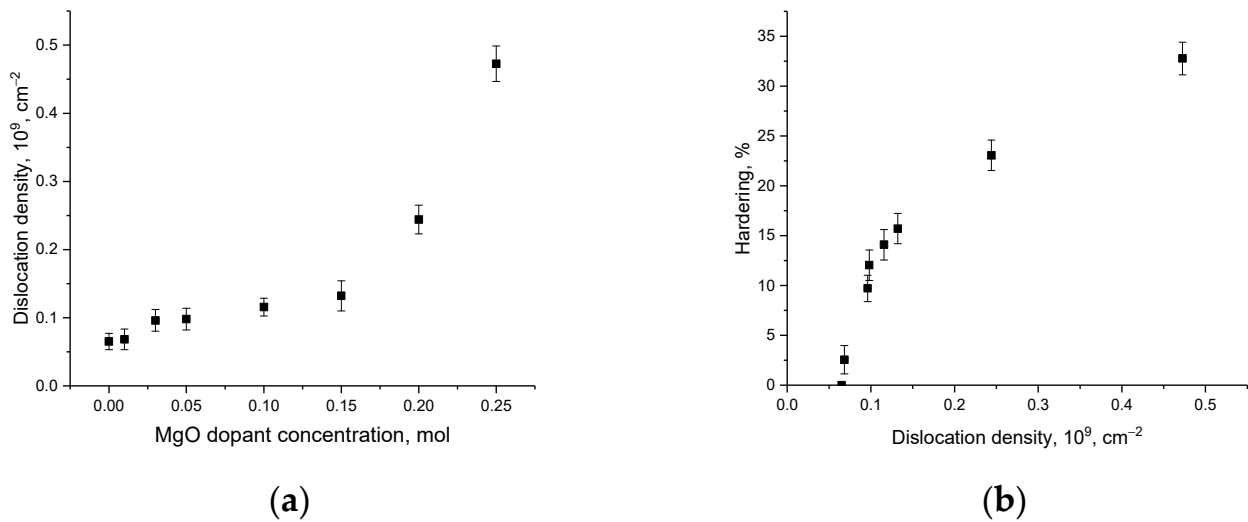


Figure 8. (a) The results of the evaluation of the dislocation density with variation in the MgO dopant concentration in ZrO_2 ceramics; (b) the relationship between hardening and change in dislocation density with a change in the morphological features of ceramics.

As can be seen from the presented data, the largest change in the dislocation density is observed for MgO dopant concentrations of 0.20–0.25 molar%, which is more than a 1.5–2-fold increase in the dislocation density. In this case, the variation in the concentration of the MgO dopant from 0.01 to 0.15 molar% does not lead to significant changes in the dislocation density. This behavior of the change in dislocation density is primarily due to size effects caused by recrystallization processes and a decrease in grain sizes associated with polymorphic transformations.

Figure 8b shows the results of the evaluation of the effect of the change in dislocation density on the hardening effect calculated based on the change in ceramic hardness values.

As can be seen from the data presented, an increase in the dislocation density above $0.1 \times 10^9 \text{ cm}^{-2}$ leads to an increase in hardening by more than 15%, while an increase in the dislocation density by more than five times (up to a value of $0.5 \times 10^9 \text{ cm}^{-2}$) at dopant concentrations leads to an increase in hardening by no more than two times. This effect indicates that with a decrease in the grain size, the so-called dislocation hardening appears, which is associated with the creation of additional obstacles for the propagation of microcracks and chips under external influences.

Figure 9 shows the results of evaluating the effects of various types of structural changes in ZrO_2 ceramics resulting from variation in the MgO dopant concentration on the hardening and change in strength properties of ceramics.

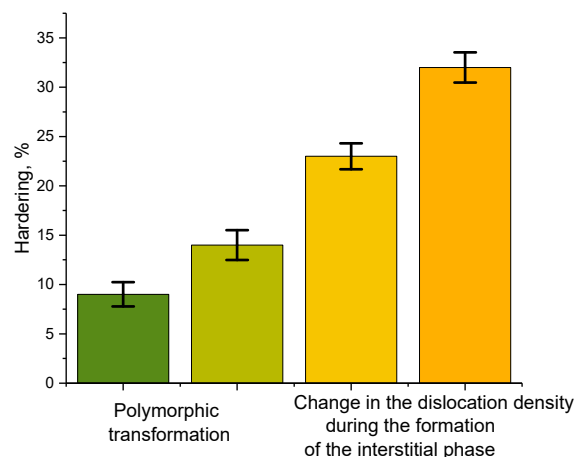


Figure 9. Influence of various factors on hardening of ceramics.

As can be seen from the presented data, polymorphic transformations of the first and the second type result in the hardening of ceramics by 10–15%, while an increase in dislocation density as a result of recrystallization processes at high MgO dopant concentrations leads to a hardening of ceramics by 25–30% in comparison with the strength properties of underperformed ceramics. Thus, it can be concluded from the obtained data that ceramic hardening is more affected by dislocation hardening than phase polymorphic transformations caused by the variation in the MgO dopant concentration. The obtained results of the influence of dopants on the resistance of ceramics to polymorphic transformations, as well as the assessment of the effects of hardening of materials, are in good agreement with several experimental studies related to the study of structural ceramics [34,35]. At the same time, in the case of composite ceramics, much attention is paid to corrosion resistance [34,36], as well as thermal resistance to sudden temperature changes [37,38], which will be the focus of the next stages of research. It should also be noted that the efficiency of ceramic hardening is associated with two factors: polymorphic transformations and dislocation hardening, of which the latter is one of the important factors used as an effective method for modifying ceramics and steels [39,40].

4. Conclusions

This paper presents the results of the study of the effect of ZrO₂ doping of MgO ceramics in the case of variation in dopant concentration as well as thermal annealing temperature. The method of mechanochemical solid-phase synthesis combined with thermal annealing of samples in an oxygen-containing atmosphere was used as a method for obtaining ceramics. An analysis of the morphological features, carried out using the method of scanning electron microscopy, showed that a variation in the MgO dopant concentration leads to a change in both the shape and size of the grains and their packing density. These changes are characteristic of recrystallization processes with a change in the phase composition of ceramics caused by polymorphic transformations with an increase in the dopant concentration. At the same time, at high dopant concentrations, the interboundary space is filled with finely dispersed MgO grains, forming a close-packed interstitial solid solution. In the case of doping of MgO samples with concentrations of 0.01–0.03 molar% during thermal annealing, a polymorphic transformation of the m—ZrO₂ → t—ZrO₂ type is observed, with the dominance of the tetragonal phase in the composition at a dopant concentration of 0.03 molar%. At MgO concentrations above 0.05 molar%, thermal annealing leads to type II polymorphic transformations t—ZrO₂ → c—ZrO₂ with complete displacement of the monoclinic and tetragonal phases in the composition of ceramics. In this case, an increase in the concentration above 0.15 molar% leads to the formation of an interstitial solid solution of the ZrO₂/MgO type, with an increase in the content of MgO phase inclusions from 3 wt.% to 17 wt.%. It was found that at high concentrations of MgO dopant making 0.20–0.25 molar%, the change in structural parameters is due to the effects associated with thermal expansion of the crystalline structure during thermal annealing. Moreover, it was determined that the incorporation of the cubic phase MgO into ceramics leads to a decrease in density, but the structural ordering degree increases. Furthermore, it was found that a change in the structural ordering degree has less effect on hardening than a change in dislocation density, which is associated with dislocation hardening with a decrease in grain size, as well as an increase in grain boundaries and the introduction of MgO grains into the intergranular space.

Author Contributions: Conceptualization, A.E.K., A.K.M., A.L.K. and A.B.; methodology, A.E.K., I.T., A.K.M., A.L.K. and A.B.; formal analysis, A.E.K., A.K.M., A.L.K. and A.B.; investigation, A.E.K., I.T., A.K.M. and A.L.K.; resources, A.E.K.; writing—original draft preparation, review and editing, A.E.K., A.K.M. and A.L.K.; visualization, I.T. and A.L.K.; supervision, A.L.K. All authors have read and agreed to the published version of the manuscript.

Funding: This research was funded by the Science Committee of the Ministry of Education and Science of the Republic of Kazakhstan (No. AP14972920).

Institutional Review Board Statement: Not applicable.

Informed Consent Statement: Not applicable.

Data Availability Statement: Not applicable.

Conflicts of Interest: The authors declare no conflict of interest.

References

1. Wei, Z.Y.; Meng, G.H.; Chen, L.; Li, G.R.; Liu, M.J.; Zhang, W.X.; Li, C.J. Progress in ceramic materials and structure design toward advanced thermal barrier coatings. *J. Adv. Ceram.* **2022**, *11*, 985–1068. [[CrossRef](#)]
2. Merino, R.I.; Laguna-Bercero, M.A.; Lahoz, R.; Larrea, Á.; Oliete, P.B.; Orera, A.; Sola, D. Laser processing of ceramic materials for electrochemical and high temperature energy applications. *Boletín Soc. Española Cerámica Vidr.* **2022**, *61*, S19–S39. [[CrossRef](#)]
3. Zvonareva, I.A.; Mineev, A.M.; Tarasova, N.A.; Fu, X.Z.; Medvedev, D.A. High-temperature transport properties of $\text{BaSn}_{1-x}\text{Sc}_x\text{O}_{3-\delta}$ ceramic materials as promising electrolytes for protonic ceramic fuel cells. *J. Adv. Ceram.* **2022**, *11*, 1131–1143. [[CrossRef](#)]
4. Yarahmadi, M.; Barcelona, P.; Fargas, G.; Xuriguera, E.; Roa, J.J. Optimization of the ceramic ink used in Direct Ink Writing through rheological properties characterization of zirconia-based ceramic materials. *Ceram. Int.* **2022**, *48*, 4775–4781. [[CrossRef](#)]
5. Zanurin, A.; Johari, N.A.; Alias, J.; Ayu, H.M.; Redzuan, N.; Izman, S. Research progress of sol-gel ceramic coating: A review. *Mater. Today Proc.* **2022**, *48*, 1849–1854. [[CrossRef](#)]
6. Al-Buriah, M.S.; Alzahrani, J.S.; Somaily, H.H.; Alrowaili, Z.A.; Olarinoye, I.O.; Saleh, H.H. Radiation shielding performance of $\text{Co}_2\text{O}_3\text{-TeO}_2\text{-Li}_2\text{O-ZrO}_2$ glass-ceramics. *J. Aust. Ceram. Soc.* **2022**, *58*, 1199–1207. [[CrossRef](#)]
7. Fu, L.; Wang, B.; Zhu, Y.; Shen, T.; Deng, Y.; Xu, G.; Xia, W. Structural integrity and damage of glass-ceramics after He ion irradiation: Insights from $\text{ZrO}_2\text{-SiO}_2$ nanocrystalline glass-ceramics. *J. Eur. Ceram. Soc.* **2023**, *43*, 2624–2633. [[CrossRef](#)]
8. Zhu, Y.; Chai, J.; Shen, T.; Niu, L.; Liu, Y.; Jin, P.; Wang, Z. Helium irradiation induced microstructural damages and mechanical response of $\text{Al}_2\text{O}_3\text{-ZrO}_2\text{-SiC}$ composites. *J. Eur. Ceram. Soc.* **2023**, *43*, 3475–3485. [[CrossRef](#)]
9. Pakseresht, A.; Sharifianjazi, F.; Esmailkhanian, A.; Bazli, L.; Nafchi, M.R.; Bazli, M.; Kirubaharan, K. Failure mechanisms and structure tailoring of YSZ and new candidates for thermal barrier coatings: A systematic review. *Mater. Des.* **2022**, *222*, 111044. [[CrossRef](#)]
10. Al-Amin, M.; Mumu, H.T.; Sarker, S.; Alam, M.Z.; Gafur, M.A. Effects of sintering temperature and zirconia content on the mechanical and microstructural properties of MgO, TiO_2 and CeO_2 doped alumina-zirconia (ZTA) ceramic. *J. Korean Ceram. Soc.* **2023**, *60*, 141–154. [[CrossRef](#)]
11. Hong, Y.; Bai, M.; Wang, S.; Chang, Q.; Zhang, X.; Zhao, X.; Wang, Y. Improved ageing-resistance and fracture toughness of zirconia-toughened alumina bioceramics via composition and microstructure design. *J. Eur. Ceram. Soc.* **2023**, *43*, 2208–2221. [[CrossRef](#)]
12. Fabregas, I.O.; Reinoso, M.; Otal, E.; Kim, M. Grain-size/(t' or c)-phase relationship in dense ZrO_2 ceramics. *J. Eur. Ceram. Soc.* **2016**, *36*, 2043–2049. [[CrossRef](#)]
13. Raveendran, S.; Kannan, S. Polymorphism and phase transitions in t- $\text{ZrO}_2/\text{CoFe}_2\text{O}_4$ composite structures: Impact of composition and heat treatments. *Cryst. Growth Des.* **2019**, *19*, 4710–4720. [[CrossRef](#)]
14. Zainuri, M. Structures and electric properties of PANI/polymorphic- ZrO_2 composites. *RSC Adv.* **2023**, *13*, 10414–10423.
15. Jin, E.; Yuan, L.; Yu, J.; Ding, D.; Xiao, G. Enhancement of thermal shock and slag corrosion resistance of MgO-ZrO₂ ceramics by doping CeO₂. *Ceram. Int.* **2022**, *48*, 13987–13995. [[CrossRef](#)]
16. Lei, W.; Luo, Z.; He, Y.; Zhang, P.; Liu, S.; Lu, A. ZrO₂-doped transparent glass-ceramics embedding ZnO nano-crystalline with enhanced defect emission for potential yellow-light emitter applications. *Ceram. Int.* **2021**, *47*, 35073–35080. [[CrossRef](#)]
17. Medvedev, P.G.; Frank, S.M.; O'Holleran, T.P.; Meyer, M.K. Dual phase MgO-ZrO₂ ceramics for use in LWR inert matrix fuel. *J. Nucl. Mater.* **2005**, *342*, 48–62. [[CrossRef](#)]
18. Deng, W.; Li, Y. High-temperature electrical properties of polycrystalline MgO-doped ZrO₂. *Mater. Res. Bull.* **2019**, *113*, 182–189. [[CrossRef](#)]
19. Wen, T.; Yuan, L.; Liu, T.; Sun, Q.; Jin, E.; Tian, C.; Yu, J. Enhanced ionic conductivity and thermal shock resistance of MgO stabilized ZrO₂ doped with Y₂O₃. *Ceram. Int.* **2020**, *46*, 19835–19842. [[CrossRef](#)]
20. Śniezek, E.; Szczerba, J.; Stoch, P.; Prorok, R.; Jastrzębska, I.; Bodnar, W.; Burkel, E. Structural properties of MgO-ZrO₂ ceramics obtained by conventional sintering, arc melting and field assisted sintering technique. *Mater. Des.* **2016**, *99*, 412–420. [[CrossRef](#)]
21. Singh, B.K.; Roy, H.; Mondal, B.; Roy, S.S.; Mandal, N. Development and machinability evaluation of MgO doped Y-ZTA ceramic inserts for high-speed machining of steel. *Mach. Sci. Technol.* **2018**, *22*, 899–913. [[CrossRef](#)]
22. Jain, M.K.; Bhatnagar, M.C.; Sharma, G.L. Effect of Pore Size Distribution on Humidity Sensing Properties of MgO doped ZrO₂-TiO₂ Ceramic. *Jpn. J. Appl. Phys.* **2000**, *39*, 345. [[CrossRef](#)]
23. Wang, J.; Zhang, L.; Chen, D.; Jordan, E.H.; Gell, M. Y₂O₃-MgO-ZrO₂ infrared transparent ceramic nanocomposites. *J. Am. Ceram. Soc.* **2012**, *95*, 1033–1037. [[CrossRef](#)]
24. Keerthana, L.; Sakthivel, C.; Prabha, I. MgO-ZrO₂ mixed nanocomposites: Fabrication methods and applications. *Mater. Today Sustain.* **2019**, *3*, 100007. [[CrossRef](#)]

25. Franco, A.R., Jr.; Pintaúde, G.; Sinatora, A.; Pinedo, C.E.; Tschiptschin, A.P. The use of a Vickers indenter in depth sensing indentation for measuring elastic modulus and Vickers hardness. *Mater. Res.* **2004**, *7*, 483–491. [[CrossRef](#)]
26. Medvedev, P.G.; Lambregts, M.J.; Meyer, M.K. Thermal conductivity and acid dissolution behavior of MgO–ZrO₂ ceramics for use in LWR inert matrix fuel. *J. Nucl. Mater.* **2006**, *349*, 167–177. [[CrossRef](#)]
27. Medvedev, P.G.; Jue, J.F.; Frank, S.M.; Meyer, M.K. Fabrication and characterization of dual phase magnesia–zirconia ceramics doped with plutonia. *J. Nucl. Mater.* **2006**, *352*, 318–323. [[CrossRef](#)]
28. Yoon, S.; Noh, T.; Kim, W.; Choi, J.; Lee, H. Structural parameters and oxygen ion conductivity of Y₂O₃–ZrO₂ and MgO–ZrO₂ at high temperature. *Ceram. Int.* **2013**, *39*, 9247–9251. [[CrossRef](#)]
29. Sathyaseelan, B.; Manikandan, E.; Baskaran, I.; Senthilnathan, K.; Sivakumar, K.; Moodley, M.K.; Maaza, M. Studies on structural and optical properties of ZrO₂ nanopowder for opto-electronic applications. *J. Alloy. Compd.* **2017**, *694*, 556–559. [[CrossRef](#)]
30. Galusek, D.; Sedláček, J.; Chovanec, J.; Micháľková, M. The influence of MgO, Y₂O₃ and ZrO₂ additions on densification and grain growth of submicrometre alumina sintered by SPS and HIP. *Ceram. Int.* **2015**, *41*, 9692–9700. [[CrossRef](#)]
31. Wang, J.; Chu, D.; Ma, H.; Fang, S.; Chen, Q.; Liu, B.; Jia, X. Effect of sintering temperature on phase transformation behavior and hardness of high-pressure high-temperature sintered 10 mol% Mg-PSZ. *Ceram. Int.* **2021**, *47*, 15180–15185. [[CrossRef](#)]
32. Nath, S.; Bajaj, S.; Basu, B. Microwave-sintered MgO-doped zirconia with improved mechanical and tribological properties. *Int. J. Appl. Ceram. Technol.* **2008**, *5*, 49–62. [[CrossRef](#)]
33. Azhar, A.Z.A.; Mohamad, H.; Ratnam, M.M.; Ahmad, Z.A. The effects of MgO addition on microstructure, mechanical properties and wear performance of zirconia-toughened alumina cutting inserts. *J. Alloy. Compd.* **2010**, *497*, 316–320. [[CrossRef](#)]
34. He, L.; Pan, L.; Zhou, W.; Niu, Z.; Chen, X.; Chen, M.; Li, Y. Thermal corrosion behavior of Yb₄Hf₃O₁₂ ceramics exposed to calcium-ferrum-alumina-silicate (CFAS) at 1400 °C. *J. Eur. Ceram. Soc.* **2023**, *43*, 4114–4123. [[CrossRef](#)]
35. Pan, L.; He, L.; Niu, Z.; Xiao, P.; Zhou, W.; Li, Y. Corrosion behavior of ytterbium hafnate exposed to water-vapor with Al(OH)₃ impurities. *J. Eur. Ceram. Soc.* **2023**, *43*, 612–620. [[CrossRef](#)]
36. Gu, S.; Zhang, S.; Xu, D.; Li, W.; Yan, J. Evolution of microstructure and hot corrosion performance of La₂Hf₂O₇ ceramic in contact with molten sulfate-vanadate salt. *Ceram. Int.* **2018**, *44*, 2048–2057. [[CrossRef](#)]
37. Sun, X.; Gong, F.; Hao, M.; Wu, L.; Yin, C.; Sun, Z.; Xiao, R. Enhanced thermal transport and corrosion resistance by coating vertically-aligned graphene on zirconium alloy for nuclear reactor applications. *Appl. Surf. Sci.* **2022**, *582*, 152484. [[CrossRef](#)]
38. Huang, J.; Wang, C.; Guo, K.; Zhang, D.; Su, G.H.; Tian, W.; Qiu, S. Heat transfer analysis of heat pipe cooled device with thermoelectric generator for nuclear power application. *Nucl. Eng. Des.* **2022**, *390*, 111652. [[CrossRef](#)]
39. Wu, S.; Kou, Z.; Lai, Q.; Lan, S.; Katnagallu, S.S.; Hahn, H.; Feng, T. Dislocation exhaustion and ultra-hardening of nanograined metals by phase transformation at grain boundaries. *Nat. Commun.* **2022**, *13*, 5468. [[CrossRef](#)]
40. Gu, L.; Meng, A.; Chen, X.; Zhao, Y. Simultaneously enhancing strength and ductility of HCP titanium via multi-modal grain induced extra-c + a dislocation hardening. *Acta Mater.* **2023**, *252*, 118949.

Disclaimer/Publisher’s Note: The statements, opinions and data contained in all publications are solely those of the individual author(s) and contributor(s) and not of MDPI and/or the editor(s). MDPI and/or the editor(s) disclaim responsibility for any injury to people or property resulting from any ideas, methods, instructions or products referred to in the content.